Distinct and conserved transcriptomic changes during nematode-induced giant cell development in tomato compared with Arabidopsis: a functional role for gene repression

Mary Portillo[1],*, Javier Cabrera[1],*, Keith Lindsey[2], Jen Topping[2], Maria Fe Andrés[3], Mariana Emiliozzi[3], Juan C. Oliveros[4], Gloria García-Casado[4], Roberto Solano[4], Hinanit Koltai[5], Nathalie Resnick[5], Carmen Fenoll[1] and Carolina Escobar[1]

[1]Facultad de Ciencias Ambientales y Bioquímica, Universidad de Castilla-La Mancha, Avenida de Carlos III s/n, 45071, Toledo, Spain; [2]Integrative Cell Biology Laboratory, School of Biological and Biomedical Sciences, Durham University, Durham, DH1 3LE, UK; [3]ICA CSIC, Protección Vegetal, Serrano 115 dpdo, 28006, Madrid, Spain; [4]Centro Nacional de Biotecnología CSIC, Darwin3, Campus Universidad Autónoma de Madrid, 28049, Spain; [5]Institute of Plant Sciences ARO, Volcani Center, 50250, Bet-Dagan, Israel

Summary

- Root-knot nematodes (RKNs) induce giant cells (GCs) from root vascular cells inside the galls. Accompanying molecular changes as a function of infection time and across different species, and their functional impact, are still poorly understood. Thus, the transcriptomes of tomato galls and laser capture microdissected (LCM) GCs over the course of parasitism were compared with those of Arabidopsis, and functional analysis of a repressed gene was performed.

- Microarray hybridization with RNA from galls and LCM GCs, infection–reproduction tests and quantitative reverse transcription-polymerase chain reaction (qRT-PCR) transcriptional profiles in susceptible and resistant (*Mi-1*) lines were performed in tomato.

- Tomato GC-induced genes include some possibly contributing to the epigenetic control of GC identity. GC-repressed genes are conserved between tomato and Arabidopsis, notably those involved in lignin deposition. However, *genes related to the regulation of gene expression diverge, suggesting that diverse transcriptional regulators mediate common responses leading to GC formation in different plant species*. TPX1, a cell wall peroxidase specifically involved in lignification, was strongly repressed in GCs/galls, but induced in a nearly isogenic *Mi-1* resistant line on nematode infection. TPX1 overexpression in susceptible plants hindered nematode reproduction and GC expansion.

- Time-course and cross-species comparisons of gall and GC transcriptomes provide novel insights pointing to the relevance of gene repression during RKN establishment.

Introduction

Root-knot nematodes (RKNs) establish an intimate interaction with their hosts, transforming four to seven differentiated root vascular cells into giant cells (GCs) that undergo mitoses without complete cytokinesis, followed by endoreduplication (Caillaud *et al.*, 2008a; De Almeida & Favery, 2011). Although the molecular basis of this transformation is not yet well understood, nematode secretions injected into the plant cells may trigger signals for GC differentiation and maintenance, some mimicking plant peptides that control proliferation/differentiation balances of stem cells from the vascular bundles, for example, the CLE-like peptides (reviewed in Rosso & Grenier, 2011) or 16D10 from RKN juveniles that interacts *in vitro* with a SCARE-CROW-like plant transcription factor (TF) (Huang *et al.*, 2006).

Drastic changes in plant gene expression occur in GCs and surrounding cells (reviewed in Gheysen & Fenoll, 2002; Escobar *et al.*, 2011; Hewezi *et al.*, 2012). Transcriptional profile changes in Arabidopsis (Hammes *et al.*, 2005; Jammes *et al.*, 2005) and tomato galls (Bar-Or *et al.*, 2005; Schaff *et al.*, 2007) reveal differences as a function of the infection time. Transcriptomic analyses during feeding cell development have only been performed in Arabidopsis and soybean for microaspirated and laser capture microdissected (LCM)-isolated syncytia in compatible interactions at early–medium infection points, revealing differences as a function of the infection stage in soybean, but not in Arabidopsis (Ithal *et al.*, 2007; Klink *et al.*, 2007; Szakasits *et al.*, 2009). However, similar analyses are still lacking for GCs. Likewise, comparisons of transcriptional profiles from excised

*These authors contributed equally to this work.

infected roots with their correspondent isolated syncytia are limited to Arabidopsis and soybean (Klink *et al.*, 2005, 2007; Ithal *et al.*, 2007). Only one study has compared expression patterns of galls with LCM GCs at 3 d post-inoculation in Arabidopsis, identifying many differentially expressed genes (DEGs) in GCs, but not in galls; thus, both structures show distinct gene expression profiles (Barcala *et al.*, 2010).

GC content isolation has been performed in mature tomato GCs (Bird & Wilson, 1994; Wang *et al.*, 2001, 2003) and also, at very early infection points (48–72h), using LCM followed by microarray hybridization (Portillo *et al.*, 2009) and followed by a cDNA library construction (Fosu Nyarko *et al.*, 2009). However, cross-species comparisons of transcriptomic data from galls/GCs or syncytia have not been reported, in spite of their potential to identify unique or conserved plant responses during plant–nematode interactions (Escobar *et al.*, 2011).

Extensive down-regulation of gene expression has been described in Arabidopsis (GCs and galls) and in tomato galls after nematode establishment, particularly of stress-related genes (Schaff *et al.*, 2007; Caillaud *et al.*, 2008b; Barcala *et al.*, 2010), suggesting the participation of putative nematode suppressors of plant defense (reviewed in Smant & Jones, 2011). For example, peroxidase-coding genes are repressed in the compatible interaction, but up-regulated in tomato *Mi* (Bar-Or *et al.*, 2005; Schaff *et al.*, 2007) and in soybean resistant plants (Klink *et al.*, 2009, 2010). The repression of particular gene subsets, such as those involved in defense and secondary metabolism, occurs in pathogenic and symbiotic interactions (Maunoury *et al.*, 2010; Schlink, 2010 Moreau *et al.*, 2011; Damiani *et al.*, 2012), but also during cell differentiation (Sawa *et al.*, 2005; Ito & Sun, 2009). In this respect, GCs have been suggested to derive from developing tracheary elements (Bird, 1996; Barcala *et al.*, 2010) through an as yet undefined nematode-triggered cell differentiation process.

To gain insight into GC and gall differentiation, we compared the differential transcriptomes of tomato LCM GCs and whole galls formed by *Meloidogyne javanica* over the course of parasitism, as well as the transcriptomes of tomato and Arabidopsis LCM GCs in the same conditions. Distinct pathways, such as those leading to lignin deposition, were highly conserved between Arabidopsis and tomato during GC development. By contrast, genes involved in the regulation of gene expression were distinct. The overexpression of a peroxidase involved in tomato lignification, TPX1, repressed in the compatible and induced in the incompatible interaction (*Mi-1*), impaired nematode feeding site development, suggesting the importance of gene repression during nematode establishment.

Materials and Methods

Plant material, nematode infections and gall sections

Seeds from tomato (*Solanum lycopersicum* Mill, cv Moneymaker) were germinated *in vitro* in Petri dishes (125 mm) on Gamborg B5 medium (Gamborg *et al.*, 1968) supplemented with 20 g l^{-1} sucrose and 1.5% agar. Each primary tomato root was inoculated just behind the root tip with sterile freshly hatched *M. javanica*

(20–30 second-stage juveniles (J2s); Portillo *et al.*, 2009; Fig. 1). Equivalent sampling and biological materials were used for all experiments, including gall hand-dissection and cryosectioning before GC LCM (Portillo *et al.*, 2009).
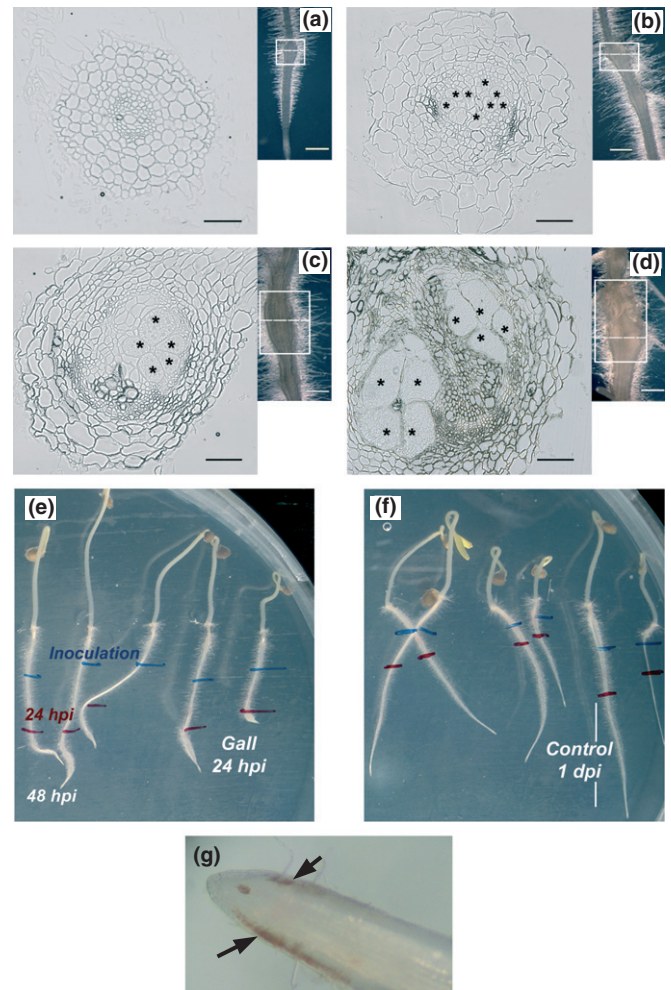
Fig. 1 Collected material and monitoring of the infection with *Meloidogyne javanica* second-stage juveniles (J2s) for expression analysis. At the top, the images on the right correspond to hand-dissected tomato galls and, on the left, their corresponding transverse Araldite® resin sections. (a–d) Tomato (*Solanum lycopersicum*) hand-dissected galls at 1, 3, 7 and 14 d post-infection (dpi) were collected. (a) The typical initial gall swelling was evident at 1 dpi (24 h post-infection; hpi). Identical experimental conditions were used to obtain giant cells (GCs) during their initiation and differentiation process: (b) at 3 dpi, the first developmental stages of GCs are clearly identified; (c) at 7 dpi, GCs are expanding and show an increase in cytoplasmic density with multiple nuclei. Section bars, 100 µm; gall bars, 1 cm. (e) As nematode penetration is not synchronous, the gall formation and position relative to the root tips were strictly monitored every 24 h. (f) Equivalent primary root tissues (in age and position) of uninfected seedlings were used as controls for the gall transcriptomic analysis and laser capture microdissection (LCM) of control tissue; the positions of the root tips were labeled every 24 h. (g) Infected root segments with necrotic areas (black arrows) from resistant *S. lycopersicum* cv Motelle (*Mi-1/Mi-1*) were collected for quantitative reverse transcription-polymerase chain reaction (qRT-PCR) 2 d post-inoculation. Equivalent root segments were also collected as controls (not shown). Asterisks in sections indicate GCs.

Seedlings of two isogenic tomato lines, susceptible Money-maker (*mi/mi*) and resistant Motelle (*Mi-1/Mi-1*) genotypes, were grown in small clay pots with 10 ml of quartz sand at $25 \pm 2°C$, 18 h light. Twenty-one-day-old plants were inoculated with 100 freshly hatched *M. javanica* J2s per plant; noninoculated plants were kept as controls (see legend to Figs 1, 7).

Transgenic *Solanum lycopersicum* cv Pera plants overexpressing the cell wall peroxidase TPX1 driven by the *35S* promoter were homozygous for a single T-DNA insertion (TP3 line; El Mansouri *et al.*, 1999; Figs 7, 8). Statistical analysis of infection and reproduction parameters after ANOVA was set to a significance level of $P \leq 0.05$ using the The SPSS statistics package, IBM (Armonk, NY, USA). Control wild-type plants were nontransformed plants from the same cultivar.

Galls at 3 and 7 dpi from *35S::TPX1* plants and controls were hand-dissected, fixed and embedded as in Barcala *et al.* (2010). Sections were stained with 1% toluidine blue in 1% borax solution (TAAB). The TrakEM2 plug-in from FIJI was used to measure the GC area (Cardona *et al.*, 2012). Two representative galls from each genotype were entirely sectioned into 2-μm slices and the areas were quantified (Fig. 8).

Gall and GC RNA isolation, amplification and aRNA probe preparation

Independent RNA extractions from 100 mg of hand-dissected galls or equivalent, uninfected controls at 1, 3, 7 and 14 dpi (Fig. 1) were performed, and the quality was assessed as in Portillo *et al.* (2006). More than 12 (uninfected plants) or 18 (infected plants) plates, each containing eight individuals, were used for each independent experiment and time point. A total of six independent experiments was performed (i.e. 3000 hand-dissected galls and 4400 uninfected root fragments). RNA from two independent experiments was pooled in equimolar ratios to obtain one 'independent biological replicate' per infection time analyzed. In total, three 'independent biological replicates' were processed. A single round of linear amplification using a MessageAmp™ II aRNA Amplification Kit (Casson *et al.*, 2005) was performed.

RNA isolation and aRNA probe preparation from LCM GCs at 3 and 7 dpi and from control vascular cells from cryosections were performed as described by Portillo *et al.* (2009). Gene annotation and putative functions for expressed sequence tags (ESTs) are described on the Solanaceae Genomics Network (SGN), http://www.sgn.cornell.edu/index.pl.

Microarray analysis

Microarray hybridization, normalization and statistical analysis of the expression data were performed as described by Portillo *et al.* (2009) and Barcala *et al.* (2010). Three or four slides were hybridized independently with aRNA from three to four independent biological replicates, including one dye-swap for both analyses: galls and LCM GCs. Two independent time points were assayed for GCs (3- and 7-dpi GCs vs their respective control cells from vascular cylinders of noninfected tissue at an equivalent developmental stage to that of the infected plants); for

galls, four independent time points were examined (1, 3, 7 and 14 dpi vs their respective noninfected root segments at an equivalent developmental stage to that of the infected plants; Fig. 1; samples and labeling in Supporting Information Table S12). Data were collected in the Cy3 and Cy5 channels. Background correction and normalization of the expression data were performed using LIMMA, as described by Adie *et al.* (2007). First, the dataset was filtered based on spot quality. A strategy of adaptive background correction was used that avoids exaggerated variability of log ratios for low-intensity spots; for local background correction, the 'normexp' method in LIMMA was used to adjust the local median background. The resulting log ratios were print-tip loess normalized for each array to have a similar distribution across arrays and to achieve consistency among arrays, and log ratio values were scaled using the median absolute value as scale estimator (Smyth & Speed, 2003). Linear model methods were used to determine DEGs. Each probe was tested for changes in expression over replicates by an empirical Bayes moderated *t*-statistic (Smyth, 2004). To overcome the problem of multiple testing, corrected *P* values (*q* values) were calculated following Benjamini & Hochberg (1995). Gene expression differences (always between galls or GCs vs their corresponding controls) were considered to be significant with $q < 0.05$. When several immobilized spots (IDs) corresponded to the same unigene (SGN-U), the representative probe with the highest differential expression level, among those with $q < 0.05$, was used for further analysis. Data from TOM1 microarray spots were downloaded from the Tomato Functional Genomics Database: http://ted.bti.cornell.edu/. Hierarchical clustering (HCL) was calculated using MultiExperiment Viewer (MeV4.1; http://www.tm4.org/mev; Saeed *et al.*, 2006) with Pearson uncentered metric distance and a complete linkage. For clustering analyses, we selected those genes with $q < 0.05$ at any of the developmental stages assayed (1, 3, 7, 14 dpi). Functional categories of DEG were obtained from the *Solanaceous* Mapman ontology for TOM1 chip. A gene was considered to be 'distinctive' of a particular developmental stage, or of galls or GCs, when it was only differentially expressed in one of the situations, but not in the other, considering a threshold of $q < 0.05$.

Real-time quantitative reverse transcription-polymerase chain reaction (qRT-PCR) and *in situ* RT-PCR

qRT-PCR was carried out as in Portillo *et al.* (2009) (primers in Table S12). Statistical analysis after ANOVA was set to a significance level of $P \leq 0.05$ using the the SPSS statistics package, IBM (Armonk, NY, USA) package.

In situ RT-PCR was performed in single 3- and 7-dpi galls (primers in Table S12). Fixation and PCR-SYBR reaction were as described in Gal *et al.* (2006). Two adjacent sections for each gall were used, one as a control PCR without primers, and repeated twice (Fig. 6). Tissues were immediately observed using a confocal microscope (Olympus IX81, Tokyo, Japan) to record the fluorescence signal (excitation and emission wavelengths of 578 and 603 nm, respectively). The BA505I filter and the argon 488-nm laser beam were modified for no fluorescence background signal in the controls.

Identification and analysis of tomato–Arabidopsis homologs

TBLASTN analysis to identify the tomato–Arabidopsis homologs was performed using, as query, AGI protein sequences of DEG from Arabidopsis 3-dpi GCs induced by *M. javanica* J2s, downloaded with 'Sequence Bulk Download and Analysis' from TAIR10 (http://www.arabidopsis.org/tools/bulk/sequences/index.jsp). The output sequences were confronted to the database TOM1 re-sequences from the 'Tomato Functional Genomics Database' (http://ted.bti.cornell.edu/cgi-bin/TFGD/array/blast.cgi; Fei *et al.*, 2011). From zero to five TOM1 probe sequences producing statistically significant alignments (E-value < 0.01) were retrieved for each Arabidopsis protein. To confirm TBLASTN matches, a reciprocal BLASTX was performed, confronting translated tomato probes with the Arabidopsis TAIR10 protein database. When the same Arabidopsis protein as in the TBLASTN analysis was matched in the BLASTX with a statistically significant value (E-value < 0.01), the genes were considered to be homologs (Table S3). It is important to note that the great majority of the considered homologs (94.4%) showed E-values $< 1E-05$. Only 2.7% of the considered homologs were chosen with E-values between 1E-02 and 1E-03. The log$_2$ ratios relative to their own controls of tomato and Arabidopsis DEG were used to obtain co-regulated and contrastingly regulated genes. The over-representation of Mapman categories within the shared genes between both species was contrasted with the chi-squared test set at $P < 0.05$.

Results

Unique gene expression profiles during tomato GC development

Transcriptomic analysis of LCM GCs at 3 and 7 dpi vs control vascular cells from uninfected roots revealed that 12% of the 8500 genes represented in the TOM1 chip were DEGs (false discovery rate cut-off, $q < 0.05$). Most genes with $q < 0.05$ also showed a fold change (FC) > 1.9. For simplicity, the terms induced/up-regulated and repressed/down-regulated are used throughout the text to mean transcript levels higher or lower than the corresponding controls, respectively.

At 3 dpi, 307 DEGs were identified, most of them down-regulated (86%). By contrast, at 7 dpi, a larger number of DEGs (1000) was obtained and the percentages of up- and down-regulated genes were similar (43.5% and 56.5%, respectively; Fig. 2a). At 3 dpi, only 51 genes were DEGs (i.e. were distinctive for this stage; see Materials and Methods). Of these, 42 (82.3%) were down-regulated. By contrast, 744 DEGs were distinctive at 7 dpi, 53.6% were up-regulated and 46.4% were repressed (Fig. 2b; Table S1).

Biologically functional information for the two GC developmental stages was obtained from *Solanaceous* Mapman ontology (Urbanczyk-Wochniak *et al.*, 2006; Fig. 3). In both GC stages, a large proportion of DEGs (323) were classified in the 'Not assigned function' category (including genes with 'No ontology' and 'Unknown function'). At 3 dpi, most DEGs in all categories were
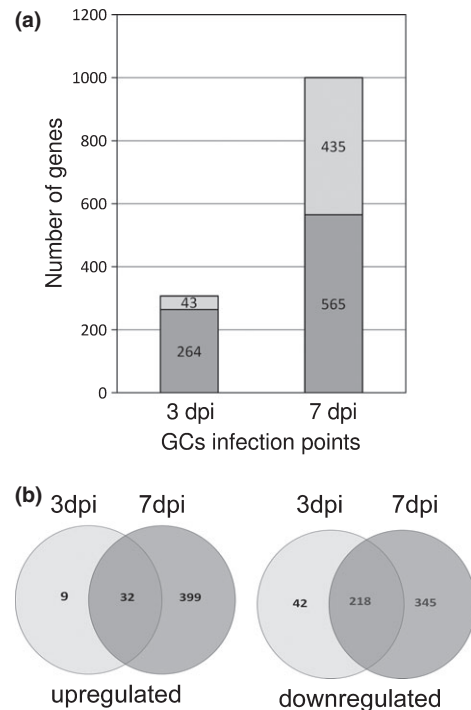

Fig. 2 Global changes in differential gene expression during tomato (*Solanum lycopersicum*) giant cell (GC) differentiation. (a) Number of differentially expressed genes (DEGs; $q < 0.05$) in laser capture microdissected (LCM) GCs at 3 and 7 d post-infection (dpi) with respect to LCM cells from the vascular cylinder of noninfected roots. (b) Venn diagrams showing temporal changes in DEGs. The intersections of the diagrams represent genes co-regulated in both infection stages. Genes that did not display a uniform expression pattern as a function of the infection time are not included in the Venn analysis, but are listed in Supporting Information Table S13. Data have been deposited at GEO, www.ncbi.nlm.nih.gov/geo (accession no. GSE30048).

clearly repressed. In the 'Stress', 'DNA', 'Cell wall' and 'Transport' categories, no induced genes were found. Similarly, at 3 and 7 dpi, most genes from the 'RNA' category (WRKY, bHLH and NAC TF families, among others) were repressed, as were 'Stress' and 'Miscellaneous' (over-represented with $P < 0.05$; Fig. 3; Table S2).

At 7 dpi, the number of DEGs increased considerably and the 'Protein' ('Protein synthesis') and 'DNA' ('DNA synthesis/Chromatin structure' and 'Histones') categories showed more induced than repressed genes (over-represented, $P < 0.05$; Fig. 3). Interestingly, genes encoding 40, 50 and 60S ribosomal proteins were up-regulated exclusively at 7 dpi. Most induced distinctive DEGs at 7 dpi (11 of 12) encoded histones, such as H3 and H4, together with genes encoding a histone deacetylase, a WD-40 repeat protein (*MSI*) putatively involved in nucleosome assembly, and a DEAD/DEAH box helicase (Dicer-like) (Table S2). Thus, the expression of genes related to chromatin remodeling, maintenance and protein synthesis is associated with particular GC developmental stages.

Conserved and nonconserved gene expression patterns in Arabidopsis and tomato GCs

The observed trends in global expression, such as large numbers of repressed genes in early developing GCs, were similar in tomato
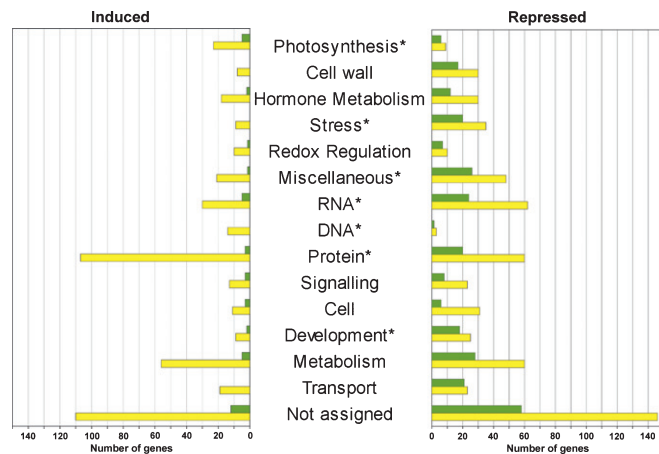
Fig. 3 Overview of differentially expressed genes in tomato (*Solanum lycopersicum*) giant cells classified into functional categories (Mapman). Bars indicate the number of genes per category. Asterisks mark categories over-represented with a statistical significance ($P < 0.05$) using the Wilcoxon Rank Sum test with Benjamini–Hochberg correction (Benjamini & Hochberg, 1995), indicative of significant differential expression profiles in comparison with the rest of the categories. Infection time points in colors as indicated.

and Arabidopsis (Barcala *et al.*, 2010; this work). Thus, we examined their putatively conserved expression patterns. We retrieved protein sequences for the 1161 Arabidopsis DEGs in LCM GCs (Barcala *et al.*, 2010) from TAIR and confronted them against the six putative open reading frames (ORFs) of the tomato database TOM1 re-sequences from the 'Tomato Functional Genomics Database' (see the Materials and Methods section) by TBLASTN (Table S3). Eight-hundred and sixty-six Arabidopsis genes matched homologous sequences in tomato. Thus, 74.6% of the Arabidopsis GC DEGs had a putative homolog protein counterpart in tomato (77% from the up-regulated and 75% from the repressed Arabidopsis DEGs). Of these, 43% were DEGs in both tomato (at 3 and 7 dpi) and Arabidopsis (at 3 dpi) GCs. Interestingly, from the 132 DEGs at 3 dpi in both species, 101 were

coordinately down-regulated (76.5%), but only one of 21 was up-regulated (0.7%; Table 1a). Similar results were observed at 7 dpi for repressed genes, whereas half of the up-regulated genes showed opposite regulation (Table 1a). In addition, a reciprocal BLASTX to confront the 482 significant counterparts found between Arabidopsis and tomato validated 93.4% (450) as the percentage of translated nucleotide sequences from tomato matching the same Arabidopsis protein sequence (E-value < 0.01; Table 1b; Table S3). An interactive spread sheet is provided to simplify searches for corresponding homologous DEGs in GCs from tomato and Arabidopsis (Table S4).

Although some caution in interpretation must be taken because of the lower unigene representation in the TOM1 microarray relative to that of Arabidopsis, genes down-regulated in early developing GCs are robustly conserved between the two species. The phenylpropanoid pathway within the 'Secondary metabolism' category was significantly over-represented among repressed genes in both tomato and Arabidopsis, particularly genes involved in lignin biosynthesis, a group of peroxidases from the category 'Miscellanea' and genes in a small biotic stress subcategory encoding protease inhibitors. These results were confirmed by an independent analysis based on different categorizations, both being highly coincident for the phenylpropanoid pathway (Table 2, Mapman; Fig. 4a, GeneOntology (GO)). When the same group of genes was placed in KEGG, all were included in the lignin biosynthesis and cross-linking routes (Fig. 4b). Thus, the down-regulation of genes encoding proteins in the lignin monomer synthesis and lignin cross-linking pathways was consistently conserved between the two species. Other over-represented categories in the GO analysis for commonly regulated genes were found, notably genes related to auxin signaling, stress responses and transport, which were also mostly down-regulated (Fig. 4a).

However, a large number of genes (Table 1a) were distinctly regulated and were not shared by tomato and Arabidopsis GCs, particularly those related to the regulation of gene expression and to housekeeping metabolic processes (Fig. 4a). In agreement with

Table 1 Giant cell differentially expressed gene (DEG) homologs

(a) TBLASTN analysis from the Arabidopsis DEGs in laser capture microdissected (LCM) giant cells (GCs) confronted to the tomato database

		Homologs in tomato*		
		3 dpi	7 dpi	3 + 7 dpi
Up-regulated genes in Arabidopsis	Same regulation in tomato	1 (0.7%)	49 (13.0%)	50 (12.7%)
	Different regulation in tomato	20 (15.1%)	55 (14.6%)	57 (14.5%)
Down-regulated genes in Arabidopsis	Same regulation in tomato	101 (76.5%)	206 (54.8%)	218 (55.6%)
	Different regulation in tomato	10 (7.6%)	66 (17.5%)	67 (17.1%)

(b) BLASTX reciprocal analysis from tomato to the Arabidopsis database

	E value range[†]				
	$< 1 \times e^{-5}$	$1 \times e^{-2} / 1 \times e^{-5}$	$> 1 \times e^{-2}$	No hit	Total significant counterparts
TBLASTN	454 (94.2%)	28 (5.8%)	–	–	482
BLASTX	436 (90.4%)	14 (2.9%)	10 (2.1%)	22 (4.6%)	450 (93.4% from those found in TBLASTN)

*Percentages and absolute data from the up- and down-regulated homologs are shown.
[†]An E-value < 0.01 was considered for significant homology.
dpi, days post-inoculation.

Table 2 Mapman functional categories of common repressed genes from the tomato and Arabidopsis giant cell transcriptomes; over-represented categories and subcategories inferred from $P < 0.05$ of the χ^2 are shown in bold

Mapman Bin			Category	χ^2	P value
6			Gluconeogenesis /Glyoxylate cycle	1.076	0.300
8			TCA/Org. transformation	0.160	0.689
9			Mitochondrial electron transport/ATP synthesis	0.000	0.983
10			Cell wall	1.105	0.293
11			Lipid metabolism	0.002	0.962
13			Amino acid metabolism	1.067	0.302
15			Metal handling	0.317	0.574
16			Secondary metabolism	3.136	0.077
	16.1		Secondary metabolism. Isoprenoids	1.068	0.301
	16.2		**Secondary metabolism. Phenylpropanoids**	**6.303**	**0.012**
		16.2.1	**Secondary metabolism. Phenylpropanoids. Lignin biosynthesis**	**7.220**	**0.007**
	16.5		Secondary metabolism. Sulfur-containing	0.057	0.811
	16.8		Secondary metabolism. Flavonoids	2.816	0.093
	16.10		Secondary metabolism. Simple phenols	0.308	0.579
17			Hormone metabolism	3.687	0.055
20			Stress	0.310	0.578
21			Redox	0.291	0.590
24			Biodegradation of xenobiotics	0.614	0.433
26			**Miscellanea**	**5.727**	**0.017**
	26.2		Miscellanea.UDP glucosyl and glucuronyl transferases	2.563	0.109
	26.7		Miscellanea.Oxidases	0.286	0.593
	26.8		Miscellanea.Nitrilases	0.286	0.593
	26.9		Miscellanea.Glutathione S transferases	1.701	0.192
	26.12		**Miscellanea. Peroxidases**	**6.218**	**0.013**
	26.13		Miscellanea.Acid and other phosphatases	2.331	0.127
	26.16		Miscellanea. Myrosinases-lectin-jacalin	0.308	0.579
	26.21		**Miscellanea.Protease inhibitor/seed storage /lipid transfer protein (LTP) family protein**	**4.251**	**0.039**
27			RNA	0.001	0.976
29			Protein	0.058	0.810
30			Signaling	2.966	0.085
31			Cell	0.155	0.694
33			Development	2.463	0.117
34			Transport	0.953	0.329

this, some TF groups, such as the b-zip, a TF family with a DNA-binding domain including a single C(2)-C(2) zinc finger (C2C2 (Zn) DOF) and another family of zinc finger TFs containing the GATA domain (GATA), or homeobox families,

did not show any gene commonly regulated between tomato and Arabidopsis (yellow label in Table S5). In addition, all TF families have either tomato or Arabidopsis homologs noncommonly regulated. However, all DEGs from lateral organ boundaries (LBDs), a transcription regulator acting as repressor of auxin-inducible gene expression (AUX/IAA) and CONSTANS like zinc finger TFs (C2C2 (Zn) CO-like) were co-regulated (Table S5).

Comparative expression profiles in tomato GCs and galls at different developmental stages

A complete transcript profile using the TOM1 microarray in galls from migration/establishment (1 dpi) to gall/GC differentiation (3 dpi) and maturity (7–14 dpi; Fig. 1) identified 2414 ESTs with significant differences ($q < 0.05$) to uninfected controls at one or more infection stages. These represent 1839 (22%) unigenes of the 8500 in the array. An interactive searching sheet is supplied that extracts gall and GC transcriptional profiles of any particular tomato ID, or from a list of IDs, at all infection stages (galls: 1, 3, 7, 14 dpi; GCs: 3, 7 dpi; Table S6).

Marked expression pattern differences as a function of the infection time were observed in galls (Fig. S1). At very early stages, most genes were down-regulated, notably at 1 dpi (71%), but also at 3 dpi (60%). As infection progressed (7 and 14 dpi), the proportion of up- and down-regulated genes was balanced (46% up, 54% down and 46% up, 54% down, respectively) and the DEG number was considerably higher than at early stages. This agrees with HCL, revealing that global transcriptional profiles between 1 and 3 dpi were more similar than those at 7 and 14 dpi, sorted in a separate cluster (Fig. 5a). At 1 dpi, 99 were exclusively DEGs, mostly down-regulated, whereas, at later stages, similar proportions of distinctive up- and down-regulated genes were observed (47–50%; Fig. S1; Tables S6, S7). A small number were DEGs during all infection stages (Fig. S1).

Significant differential expression profiles ($P < 0.05$) were encountered in the 'Cell wall' category, as the induced gene number increased over the infection course. By contrast, the percentage of repressed genes in the 'Stress' category (23%) was markedly high at 1 dpi, but lower at later time points (Fig. S2). Hence, of the 99 distinctive genes at 1 dpi (Table S7), 66 were in the 'Stress' category. DEGs with expression level variations at different infection points are listed in Table S8.

To study differences between gene expression changes in GCs and galls, we compared their differential transcriptomes in samples obtained with equivalent biological sampling, using the same microarray platform, at the same developmental stages (3 and 7 dpi) and with the same data analysis tools. Each time point was compared independently, but cross-comparisons between analyses were also considered. Less than half of GC DEGs at 3 and 7 dpi were also detected as gall DEGs (148 of 307 and 469 of 1000, respectively). This indicates that many DEGs were GC distinctive (Fig. 5; Table S9). Distinctive GC DEGs at 3 dpi were predominantly down-regulated, whereas, at 7 dpi, the proportion of up- and down-regulated GC-distinctive genes was balanced (Fig. 5). When all co-expressed GC and gall DEGs were compared, the $\log_2$ values of their expression values were generally
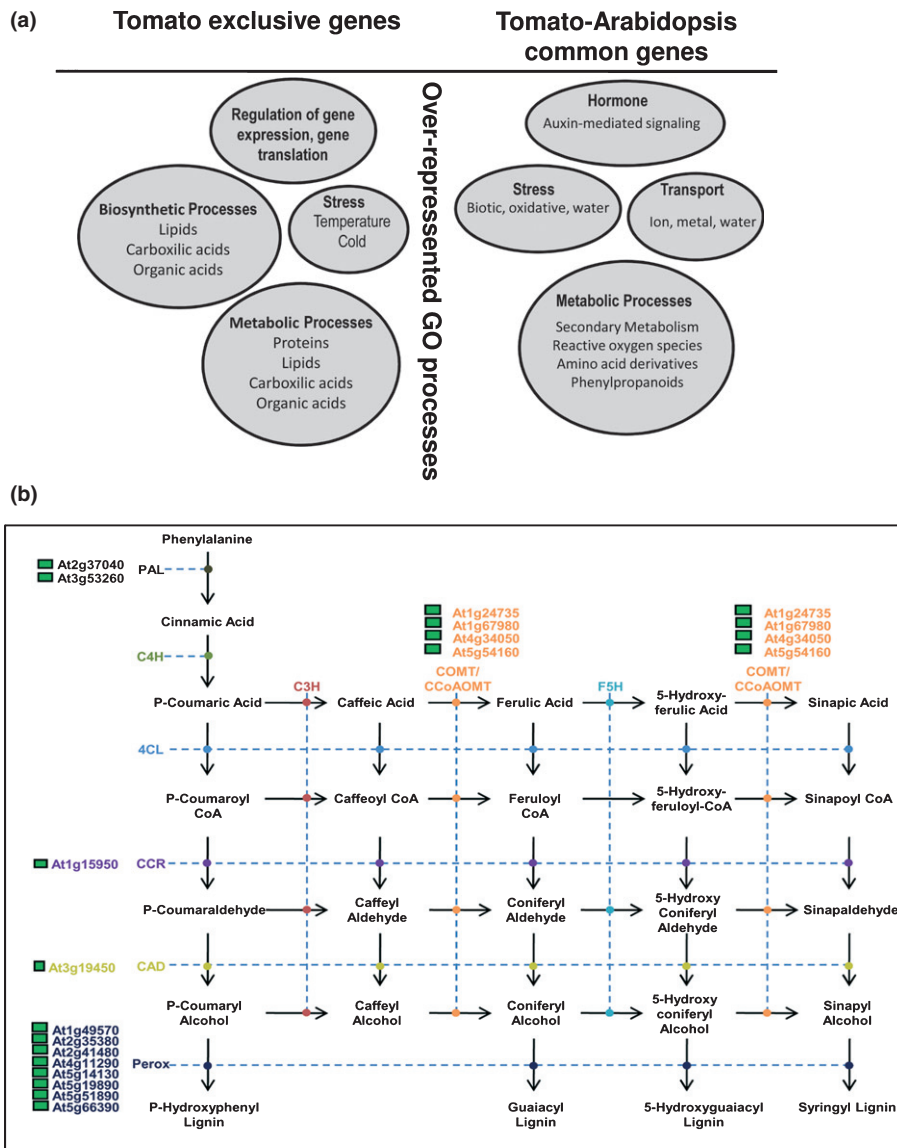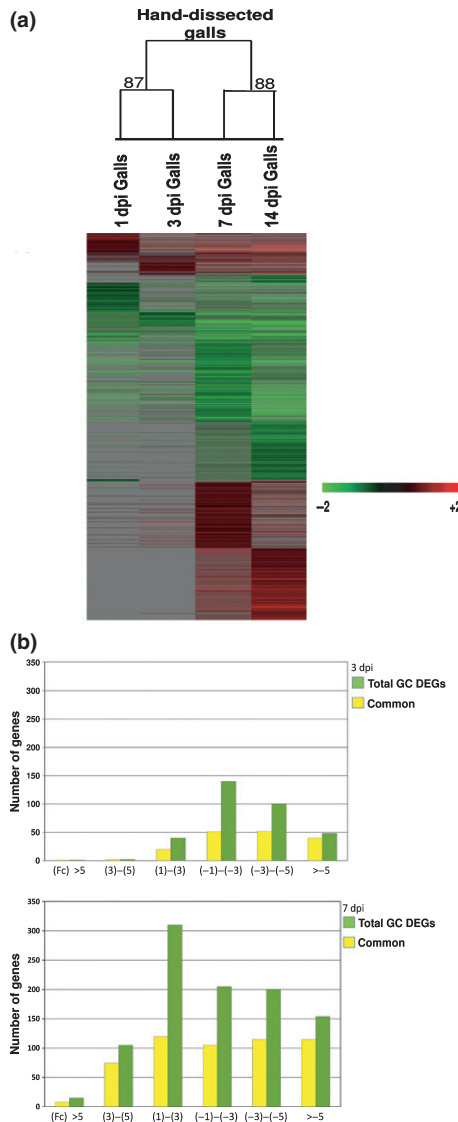
Fig. 4 Comparison of tomato (*Solanum lycopersicum*) and Arabidopsis giant cell (GC) transcriptomes. (a) Categorization of tomato–Arabidopsis homologs following GeneOntology (GO) processes. Only over-represented categories (with $P < 0.05$ from the χ^2) of the commonly regulated and exclusive (not co-regulated in both plant species) genes are shown. (b) Adapted pathway from KEGG for lignin biosynthesis and cross-linking enzymes. Genes represented are the conserved homologs between tomato and Arabidopsis in GCs. Green squares, repressed genes.

lower in galls than in GCs (Table S9). A group of distinctive GC genes (eight at 3 dpi and 276 at 7 dpi) was obtained when all DEGs from galls at 1, 3, 7 and 14 dpi were compared with those of 3- and 7-dpi LCM GCs (Table S10).

Functional classification of distinctive gall and GC genes expressed at the same developmental stage revealed differences in the predominant biological processes altered. The largest number of distinctive genes was classified in the 'Not assigned' category (Fig. S3; Table S9). At 3 dpi, GC-distinctive genes were mostly repressed (grouped in 'Stress', 'RNA', 'Protein', 'Secondary metabolism' and 'Transport'), whereas gall-distinctive genes were mostly induced (Fig. S3), essentially for the categories 'RNA: regulation of transcription' and 'Protein: protein degradation'. Interestingly, the 'Stress' category contained a high proportion of induced genes in galls in contrast with GCs. 'Miscellaneous' was the group with the largest number of distinctive up-regulated genes in galls and down-regulated genes in GCs, encoding proteins such as glucosyltransferases and peroxidases, among others (Fig. S3).

At 7 dpi, 'Protein', 'Metabolism', 'RNA' and 'Miscellaneous' categories showed the highest number of distinctive GC and gall genes. Eleven members of the histone family were solely induced in 7-dpi GCs, none being differentially expressed in either 7-dpi galls or 3-dpi GCs. Other genes putatively involved in chromatin structure maintenance or remodeling, such as *SNF2,* seem to be distinctive of 3-dpi GCs (Fig. S4; Table S9). The subcategory 'Protein synthesis', containing genes encoding ribosomal proteins, included a large number of DEGs, in both galls and GCs, but encoded different proteins (Table S9). One of the major categories of distinctive genes in GCs and galls at both developmental stages was 'RNA', containing mainly TFs that could be key regulators of cell differentiation. A detailed analysis of the 'Regulation of transcription' subcategory showed all members of TFs containing the WRKY domain, WRKYGQK, (WRKY) and the basic helix-loop-helix (bHLH) families repressed in GCs, but not in galls. Most AP2 (APETALA2) and EREBPs (ethylene-responsive element

Fig. 5 Time course of transcript profiles of tomato (*Solanum lycopersicum*) galls and comparison between differentially expressed genes (DEGs) of giant cells (GCs) and galls. (a) Hierarchical cluster analysis of tomato gall DEGs at 1, 3, 7 and 14 d post-infection (dpi). The numbers within the tree correspond to the bootstrap values after 1000 iterations. (b) Total DEGs in GCs and those common to galls. The number of 'GC-distinctive genes' increased in the lower fold change (FC) ranges.

binding proteins), AP2/EREBP, and all members of a TF family containing the no apical meristem, NAM, domain (NAC) were repressed in galls and GCs at both stages. Some members of the homeobox domain TFs (HB), C2C2 (Zn) DOF and GATA zinc finger families, among others, were up-regulated in galls, but not in GCs. Interestingly, repression levels were less pronounced in galls than in GCs, suggesting that GCs contribute strongly to the gene repression found in galls (Fig. S4).

Another category showing clear differences between GCs and galls was 'Metabolism'. All genes associated with lipid, amino acid and secondary metabolism were repressed in GCs at 3 and 7 dpi, but most were either induced or not DEGs in galls. Similarly, most biotic stress-related genes were repressed in GCs at 3

and 7 dpi, but induced in galls, including those encoding pathogenesis-related proteins (e.g. in Tables S9, S11). These patterns indicate that GCs and the other gall tissues exhibit independent and differential transcriptional profiles.

Confirmation of microarray data

qRT-PCR was performed for 15 genes, selected by criteria such as similar expression profiles over infection time, high FC or preferentially expressed in galls or GCs (primer sequences in Table S12). The reference gene for normalization encoded a hypothetical protein (SGN-U150992, 1-1-6.4.11.14) and showed steady expression as a function of the infection time in galls and GCs. qRT-PCR revealed transcriptional patterns similar to those found in microarray hybridization; only one gene coding an omega-6 fatty acid desaturase showed a different expression pattern at 7 dpi in galls with both methods (underlined in Table 3). Some were not DEGs in the microarray at certain infection points (white boxes in Table 3), although a clear tendency to up- or down-regulation was observed, coincident with qRT-PCR data.

In situ RT-PCR hybridization for selected genes preferentially expressed in GCs (40S ribosomal protein (*40S*) and a putative serine/threonine kinase (*STK*)) revealed that both accumulated in 7-dpi GCs (Table 3; Fig. 6b,d), but not in their corresponding controls (Fig. 6a,c). In agreement with the GC induction of 40S and *STK* from the microarrays (Table 3), the signal observed by *in situ* PCR in GCs was absent or much lower in adjacent cells (Table 3; Fig. 6b,d), regardless of the differences in detection sensitivity. Transcripts for the same genes in control uninfected roots were barely detectable; an example is provided for *STK* in Fig. S5. Hence, the high validation rate of the microarray data with qRT-PCR, combined with the *in situ* RT-PCR, reflects a significant reliability of the transcriptomic data.

Functional characterization of a tomato GC-repressed peroxidase

To elucidate the biological relevance of early gene down-regulation in galls and GCs, particularly of genes involved in lignin deposition, during compatible interactions, we used tomato plants over-expressing the basic cell wall peroxidase TPX1. *TPX1* was consistently down-regulated in tomato galls from early stages (1 dpi) at the infection points analyzed and strongly down-regulated in GCs (3 and 7 dpi; FCs of − 2.7 and −4.6, respectively; Table 3). In Arabidopsis GCs, 10 peroxidase-coding genes were repressed; eight had tomato homologs, all co-repressed in tomato and Arabidopsis GCs. These included four putative Arabidopsis homologs of TPX1 (ID: 1-1-3.2.20.9) (AT2G35380; AT2G41480; AT4G11290; AT5G51890; Fig. 4). TPX1 has been formerly characterized as being directly involved in lignin biosynthesis in tomato (El Mansouri *et al.*, 1999).

We first analyzed *TPX1* expression in a homozygous resistant line (Motelle, *Mi-1/Mi-1*) triggered by *M. javanica* 2 d after inoculation when compared with a nearly isogenic tomato susceptible line (Moneymaker, *mi-1/mi-1*; Schaff *et al.*, 2007). The results

Table 3 Quantitative reverse transcription-polymerase chain reaction (qRT-PCR) validation of gall microarray hybridization data

Description	Relative expression levels ($\log_2$)									
	Galls 1 dpi		Galls 3 dpi		Galls 7 dpi		Galls 14 dpi		GCs 3 dpi	GCs 7 dpi
	qPCR	Array	qPCR	Array	qPCR	Array	qPCR	Array	Array	Array
Putative LRP (lateral root primordia) 1	2.03	0.90	2.40	1.67	2.40	1.96	2.49	2.48	1.71	1.85
Wound-induced protein Sn-1	1.33	0.08	2.82	2.74	3.83	4.08	3.54	4.47	1.95	−0.44
Late-embryogenesis protein lea5	−0.95	−1.83	−0.65	−2.00	−1.78	−1.58	−1.41	−1.71	−3.34	−4.31
Xyloglucan endotransglycosylase (XTR4)	−1.63	−1.22	−1.47	−1.69	−2.31	−1.65	−1.98	−3.03	−2.49	−2.98
Pathogenesis-related protein PR-1 precursor	−1.52	−2.05	−0.81	−1.09	−2.57	−1.45	−2.00	−1.99	−2.82	−4.63
Peroxidase (TPX1)	−0.51	−1.13	−0.64	−0.97	−1.15	−2.29	−2.25	−2.66	−2.68	−4.58
Omega-6 fatty acid desaturase	0.14	0.27	1.59	0.71	−1.13	1.04	−2.14	1.02	1.44	2.29
Histone H3 [Arabidopsis thaliana]	−0.28	−0.45	−0.09	−0.23	1.07	−0.11	0.99	1.45	0.20	3.01
HD-Zip transcription factor Athb-14 (HD)	−0.28	−0.04	0.74	0.26	2.20	1.10	1.87	0.85	2.37	1.66
WRKY family transcription factor	1.35	0.85	1.81	1.34	1.54	1.51	1.75	1.66	1.05	−0.55
Homeotic protein VAHOX1 - tomato	−0.89	−0.75	−0.26	−0.69	−0.60	−0.44	0.18	−0.83	−1.04	−1.37
Receptor protein kinase-related protein [Arabidopsis thaliana]	0.68	0.71	1.85	1.07	0.14	1.15	1.27	1.07	0.96	−0.26
Putative serine/threonine kinase similar to NAK (STK) *	0.40	0.09	0.42	0.33	0.003	0.58	1.38	0.55	1.20	1.45
40S ribosomal protein S17 (40S) *	0.73	0.35	−0.17	0.01	0.32	0.40	0.32	0.54	0.22	1.13
Expansin precursor	3.64	0.17	3.48	0.67	2.03	1.51	2.03	1.51	0.36	−0.22

The columns indicate the means of qRT-PCR data from three independent biological replicates ($P < 0.05$) and microarray $\log_2$ ratios of differentially expressed genes (DEGs) from galls and giant cells (GCs) at 1, 3, 7 and 14 dpi vs their corresponding uninfected primary root fragments and laser capture microdissected (LCM) vascular cells, CCs, respectively, taken as controls. Green squares, repressed genes (−) and red squares, induced genes (+), with $q < 0.05$. White boxes represent no DEGs ($q > 0.05$) from the microarray at the infection points indicated. Those data with opposite expression in qRT-PCR relative to the microarray are underlined.
*Genes also tested by *in situ* PCR.
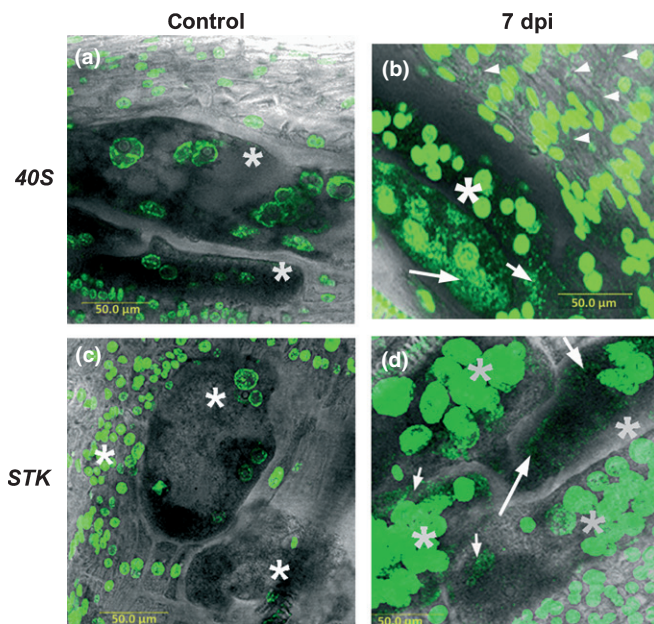
Fig. 6 *In situ* reverse transcription-polymerase chain reaction (RT-PCR) hybridization in longitudinal sections of tomato (*Solanum lycopersicum*) giant cells (GCs) at 7 d post infection (dpi). *40S*, ribosomal protein S1; *STK*, putative serine/threonine kinase. Asterisks indicate GCs. (a, c) Sections with control reactions, no primers added. (b, d) Specific amplification signals are observed as SYBR fluorescence in the GC cytoplasm (long white arrows). Fluorescence of the nuclei also corresponds to SYBR, as it nonspecifically binds double-stranded DNA (Gal *et al.*, 2006). Hence, only cytoplasmic label corresponds to specific transcript signals. Bars, 50 µm. Fluorescence in the cytoplasm of cells adjacent to GCs (short white arrows in b).

confirmed the repression observed in the microarray for the compatible interaction (Fig. 7a). By contrast, a remarkable induction (above nine-fold) was observed during the incompatible interaction (Motelle; Fig. 7a); both infection-site RNAs were compared against their noninfected controls (see Materials and Methods). These data indicate a contrasting behavior of *TPX1* during RKN compatible and incompatible interactions in tomato.

Subsequently, infection tests were performed in a homozygous TPX1-overexpressing line (TP3) from a tomato susceptible cultivar, *Solanum lycopersicum* cv Pera, carrying a single T-DNA insertion, which showed apparently normal root growth *in vitro*, but exhibited peroxidase activity and lignin content higher than controls. It was selected among three independent lines because it presented the highest peroxidase activity (El Mansouri *et al.*, 1999). In TP3, nematode infection was severely impaired, as shown by the significantly reduced number of galls formed per plant (*c.* 35% reduction compared with wild-type controls; $P < 0.05$; Fig. 7b). Nematode reproduction parameters, such as the number of eggs and number of egg masses/root dry weight, were strongly affected (35 and 25% reduction, respectively Fig. 7d,e). The number of egg masses/gall was also reduced (35% reduction, Fig. 7c). Consistently, galls in which the nematode had successfully established showed less expanded GCs than control galls at 3 and 7 dpi (Fig. 8a). GC areas in gall sections showed significant differences ($P < 0.05$) between the nontransgenic control and the TPX1-overexpressing line (*TPX1-OE*) at both infection stages, with more than a four-fold variation at 7 dpi (Fig. 8b).
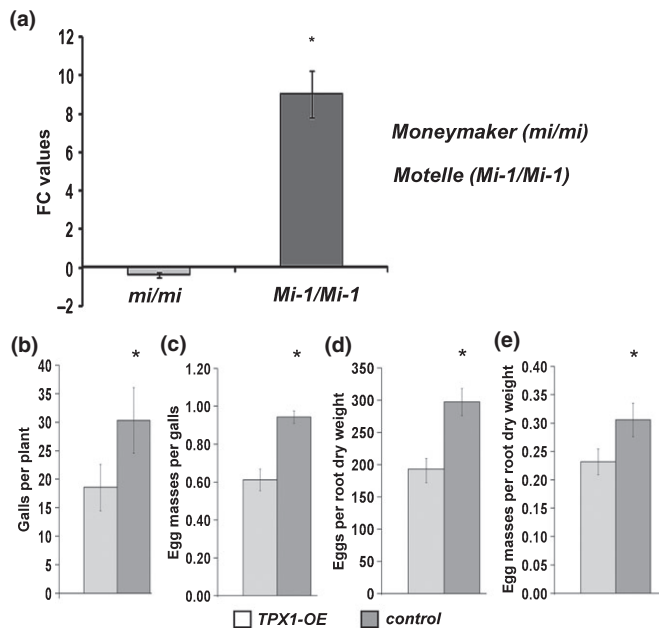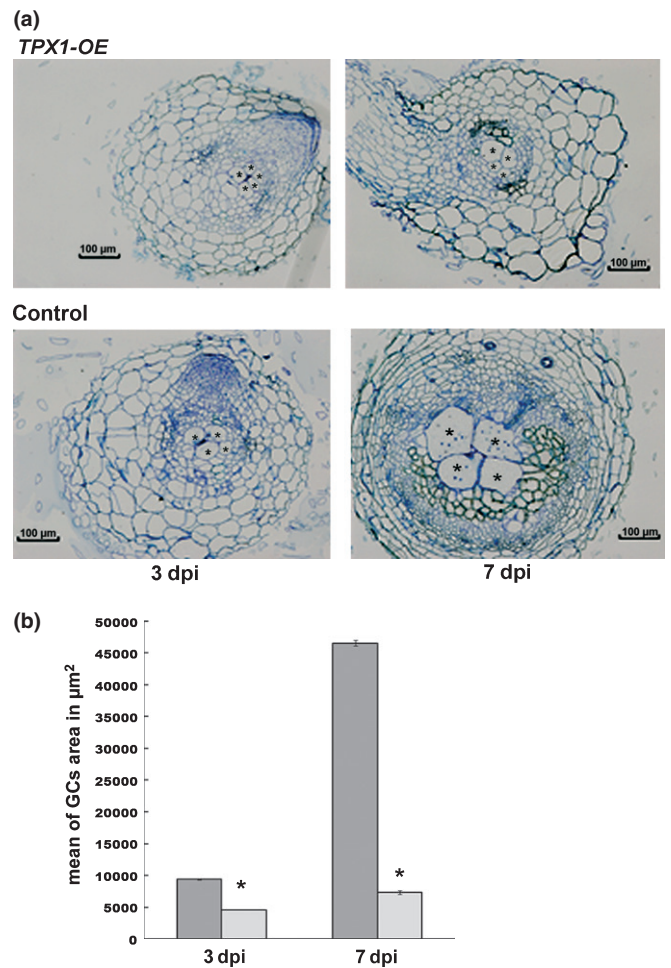
Fig. 7 Functional analysis of tomato (*Solanum lycopersicum*) peroxidase TPX1. (a) Fold change (FC) values after quantitative reverse transcription-polymerase chain reaction (qRT-PCR) of *TPX1* transcripts from susceptible (Moneymaker; *mi/mi*) and resistant (Motelle, *Mi-1/Mi-1*) nearly isogenic lines infected with *Meloidogyne javanica* second-stage juveniles (J2s). Bars indicate standard errors from three independent experiments with at least 10 plants each. Infection sites were hand-dissected 2 d after inoculation together with equivalent root segments from uninfected plants. (b–e) Infection and reproduction parameters in TPX1-overexpressing plants (*TPX1-OE*) relative to wild-type controls, both *Solanum lycopersicum* cv Pera. The number of galls per plant was assessed at 7–15 d after inoculation and reproduction parameters (number of egg masses per galls, number of eggs and egg masses per root dry weight) at 60–70 d after inoculation. The root dry weight was used to normalize most of the parameters measured. Data are representative from six independent *in vitro* experiments. Standard errors are represented. Asterisks mark statistically significant differences (*P* < 0.05) between *TPX1-OE* and wild-type controls.

Fig. 8 Functional analysis of tomato peroxidase TPX1 in tomato (*Solanum lycopersicum*) plants. (a) Ten-micrometer representative sections of fixed galls from wild-type controls and TPX1-overexpressing plants (*TPX1-OE*) in a susceptible cultivar, *S. lycopersicum* cv Pera. Asterisks mark giant cells (GCs); bars, 100 μm. (b) Average of the total area occupied by GCs from consecutive gall sections measured for two independent representative galls of *TPX1-OE* and wild-type controls at each infection point (dpi, days post-infection). Bars indicate standard errors from seven sections. Asterisks mark statistically significant differences (*P* < 0.05) between *TPX1-OE* and wild-type controls.

Discussion

A comprehensive examination of the still poorly understood transcriptional events associated with GC differentiation in crops, such as tomato, may reveal information relevant for nematode control. This is the first time that differentially expressed transcripts of GCs from equivalent developmental stages have been compared between Arabidopsis and tomato, under the same experimental conditions and data processing. This approach identified a group of genes consistently down-regulated in Arabidopsis and tomato feeding sites; among them is a peroxidase, TPX1, with a contrasting behavior in compatible and incompatible interactions. TPX1 overexpression in a susceptible cultivar severely interfered with RKN infection and reproduction.

Comparative expression profiles of tomato GCs and galls at different developmental stages

A clear boundary was found in the molecular changes detected between the initial stages of nematode infection (1–3 dpi) and

the later stages of gall development (7–14 dpi, Figs S1, S2). The percentage of repressed genes was close to 71% in early stages, but only *c.* 50% in later stages, in accordance with the observed changes in GCs (Fig. 2). This indicates that transcriptional changes during the first stages of nematode infection include the selective down-regulation of transcription, perhaps to allow initial migration/establishment, appropriate GC induction and gall formation (Schaff *et al.*, 2007).

When tomato GC and gall differential transcriptomes at the same developmental stages (3 and 7 dpi) and from the same experiments were compared, many DEGs in GCs were not DEGs in galls (Figs 5, S3), in agreement with Arabidopsis galls/GCs at 3 dpi (Barcala *et al.*, 2010). This suggests that tomato GC differentiation also requires specific transcriptional changes different from the rest of the gall.

One of the categories with contrasting expression between GCs and their corresponding galls is 'Stress', with a high proportion of genes repressed in GCs, but not DEGs or induced in galls (i.e. pathogenesis-related proteins, PRPs; Fig. S3; Table S9), in accordance with previous observations in Arabidopsis GCs (Barcala et al., 2010) and tomato galls at 1, 5 and 10 dpi (Bar-Or et al., 2005; Bhattarai et al., 2008). The vast majority of 'Stress' genes either co-expressed in GCs and galls, or GC distinctive, were repressed (Table S9), suggesting that nematodes trigger a defense response in galls different from their GCs. Other obligate biotrophic pathogens, such as phytopathogenic bacteria (Truman et al., 2006; Aslam et al., 2008), biotrophic and hemibiotrophic fungi (Cooper et al., 2008) and symbiotic microorganisms (Maunoury et al., 2010; Damiani et al., 2012), can disable host defenses. Although putative nematode suppressors of plant defense have been suggested (Hewezi et al., 2010; reviewed by Smant & Jones, 2011), knowledge on the mechanisms governing this suppression is still sparse. Consistent with all of these observations, we found that the vast majority of genes encoding TFs and enzymes related to chromatin modification were GC distinctive and not similarly regulated in galls (Figs S3, S4; Table S9).

Reprogramming GCs in tomato

Within developing GCs, 1051 transcripts were differentially expressed vs vascular control LCM cells from noninfected roots. The DEG number increased at 7 dpi, suggesting increased transcription complexity between 3 and 7 dpi (Fig. 2). At 7 dpi, 64 of 65 genes classified in 'Protein synthesis', encoding mainly ribosomal proteins and translation elongation factors, were up-regulated, in agreement with other transcriptomic studies in tomato and Arabidopsis galls (Jammes et al., 2005; Schaff et al., 2007; Bhattarai et al., 2008; Tables S1, S2). This could be related to the higher transcription rate and increased protein synthesis needed for GC differentiation and growth (Bird, 1961).

One of the first detectable signs of GC initiation is nuclear division with partial cytokinesis, the number of nuclei per GC nearly doubling during each of the first 4 d after infection (Starr, 1993; Caillaud et al., 2008a). Functional and expression analyses of CCS52 (a cell cycle switch promoting endoreduplication) indicate that endoreduplication takes place in early-developing GCs (reviewed in De Almeida & Favery, 2011). G1/S transition and S-phase genes, that is, those coding for histones, minichromosome maintenance (MCM) proteins and DNA helicases, were up-regulated in tomato GCs (Tables S1, S2). MCM proteins are part of a complex that regulates DNA replication initiation (Shultz et al., 2007). In Arabidopsis, the MCM family member PROLIFERA (PRL) was expressed in GCs from the earliest developmental stages (Huang et al., 2003). Furthermore, the expression of 11 histone-coding genes increased between 3 and 7 dpi, notably the core histones H3 and H4 (FCs of 8 and 11, respectively; Table S2). H4 deposition and modification have been related to cell proliferation, and this is a well-characterized gene up-regulated during the G1/S transition (Sanchez et al., 2008).

Particularly relevant is a set of induced genes that might regulate the GC differential expression pattern and cellular identity, as their products are involved in chromatin remodeling and transcriptional control. Among them are members of the NF-Y gene family of TFs with putative roles in cellular differentiation (Siefers et al., 2009), induced from 3 dpi and increasing at 7 dpi. Likewise, the only member of the MYB family induced in GCs is a homolog of PHANTASTICA, involved in leaf organogenesis and cell differentiation, as reported in tomato and Medicago truncatula GCs (Koltai & Bird, 2000; Koltai et al., 2001). Other genes encode a chromomethylase (CMT) involved in DNA methylation (Lindroth et al., 2001), proteins related to histone methylation and deacetylation (HDAC), matrix-attachment region (MAR)-binding proteins, MSI (multicopy suppressor of ira1) proteins important for chromatin organization, condensation or modification (Hollender & Liu, 2008) and a DICER-LIKE coding gene with functions in the miRNA-mediated silencing machinery, all highly expressed in GCs (Tables S1, S2, S6; Fig. S4; Kohler et al., 2003). These proteins can influence processes correlated with gene silencing and are key to the maintenance of epigenetic gene expression patterns (Smith et al., 2007; Knizewski et al., 2008), and their induction might be related to the observed large-scale gene repression during feeding site development. Recent analyses have reported several nematode-secreted proteins with putative nuclear localization, DNA binding or chromatin modification domains, one directly localized in the nucleus (Bellafiore et al., 2008; Jaouannet et al., 2012). In agreement with these observations are those obtained in the Arabidopsis GC transcriptome (Barcala et al., 2010). All this evidence indicates that the output of secreted nematode effectors might be a series of dynamic changes in chromatin structure. As these processes are necessary for cell identity and differentiation, they might participate in the triggering of GC fate in its initials, developing root vascular stem cells. In addition to these genes up-regulated in GCs, the data suggest that transcriptional reprogramming of GCs acts in concert with large-scale gene repression, particularly obvious at 3 dpi (Fig. 2). For example, genes encoding TFs from the WRKY, bHLH and NAC families, involved in stress responses or in secondary wall thickening (Toledo-Ortiz et al., 2003; Olsen et al., 2005; Eulgem & Somssich, 2007; Zhong et al., 2008), were all repressed in 3- and 7-dpi GCs (Fig. S4; Table S5).

Down-regulation of gene expression in RNK feeding sites is conserved in Arabidopsis and functionally relevant in tomato

It is generally accepted that one of the first events in feeding site formation is the reprogramming of developmental fate in vascular cells towards GC identity (Williamson & Hussey, 1996). Although some evidence was provided by meta-analysis of transcriptomic data (Barcala et al., 2010), no demonstration of the molecular events during successful GC formation from vascular initials has been provided to date. According to our GC-specific transcriptome at very early stages, part of this reprogramming could rely on large-scale repression of gene expression (Fig. 2;

Table 1). Gene down-regulation has been described in *Arabidopsis* and tomato gall transcriptomes at mid–late infection stages and from the expression analysis of several gene promoters, but evidence has been focused mainly on stress-related genes, as also observed in this study (Caillaud *et al.*, 2008b; Fig. S3). For example, all WRKYs with a putative tomato–Arabidopsis homolog were repressed, either co-regulated or not (Table S5). Although, none was identified as WRK72a or b, both involved in basal resistance in tomato and also related to *Mi-1*-dependent immunity (Bhattarai *et al.,* 2010), the data are in agreement with plant defense suppression in GCs. Recently, the repression of defense-related genes has been suggested as a common target for rhizobia and nematodes at the cellular level (Damiani *et al.*, 2012). We present the first direct molecular evidence that transcriptional repression patterns are highly conserved in early phases of GC development in tomato and Arabidopsis, as 76.5% of the tomato–Arabidopsis homologs found in TOM1 were co-repressed in both species, whereas only 0.7% were co-induced in 3-dpi GCs (Table 1).

In silico comparison revealed that genes from the phenylpropanoid pathway, coding enzymes involved in lignin biosynthesis and deposition, were significantly over-represented, considering the genes with a corresponding counterpart in Arabidopsis and tomato GCs, consistently in three independent analyses (Table 2; Fig. 4). Phenylpropanoids are a widely diverse group of molecules, some involved directly in plant defenses, such as salicylic acid (SA) (Chen *et al.*, 2009; Fraser & Chapple, 2011). However, all phenylpropanoid-related DEGs in tomato and Arabidopsis were found in the same lignin precursor biosynthesis route, but none was involved in the synthesis of other secondary metabolites, such as SA or flavonoids, down-stream from cinnamic acid and feruloyl-CoA (Chen *et al.*, 2009; Fraser & Chapple, 2011; Fig. 4). Furthermore, many genes down-regulated in GCs (3–7 dpi) and in early-developing galls (1–3 dpi, but not at 7–14 dpi) play a direct role in lignin content and composition, demonstrated through mutant analysis in Arabidopsis (as genes encoding cinnamate-4-hydroxylase (C4H), 4-coumarate: CoA ligase (4CL), p-coumarate 3-hydroxylase (C3H), caffeoyl CoA 3-O-methyltransferase (CCoAOMT), cinnamoyl-CoA reductase (CCR), ferulate 5-hydroxylase (F5H) and caffeic acid O-methyltransferase (COMT); Fraser & Chapple, 2011; Fig. 4). Repression of this particular group of genes might be crucial for appropriate gall and GC formation at the initial stages. Furthermore, plant peroxidases are highly diverse and grouped into several classes (PeroxiBase; Passardi *et al.*, 2007); some have been demonstrated to participate directly in lignin cross-linking in Arabidopsis (Almagro *et al.*, 2009). In tomato, TPX1 mediates a late step in lignin monomer cross-linking (Lucena *et al.*, 2003), and was drastically and consistently repressed in GCs and galls as a function of the infection time from the early stages (Table 3). Moreover, nematode infection and reproduction were severely impaired in *TPX1*-overexpressing tomato susceptible plants, as was GC expansion (Figs 7, 8). However, genes involved in the phenylpropanoid pathway and some peroxidases were up-regulated in susceptible soybean syncytia from early to medium infection stages (Ithal *et al.*, 2007; Klink *et al.*, 2007) and during the

resistance phase in resistant soybean (Klink *et al.*, 2009, 2010). By contrast, peroxidases were repressed in Arabidopsis syncytia at 5 and 15 dpi (Szakasits *et al.*, 2009). Contrasting results from syncytia could indicate differential regulation depending on plant species or may require more detailed analysis. However, in tomato and Arabidopsis GCs, *TPX1* and its homologs, as well as genes for lignin biosynthesis, were consistently repressed (Fig. 4, Table 3), and may be necessary for gall and/or GC differentiation. Further support for this interpretation is that *TPX1* transcripts were highly induced in infected *Mi-1* resistant plants relative to the susceptible *mi-1* line (Fig. 7), which agrees with the assumption that peroxidase repression is characteristic of tomato–nematode compatible interactions relative to incompatible interactions involving resistant *Mi-1* genotypes (Schaff *et al.*, 2007).

The repression of particular signaling cascades occurs during cell differentiation (Sawa *et al.*, 2005; Ito & Sun, 2009). RKN secretions, such as the CLE-like 16D10 peptide, may play a role in GC formation from procambial cells by restricting their differentiation into xylem elements (reviewed in Gheysen & Fenoll, 2011). Moreover, GCs might also arise from partially differentiated tracheary elements (Bird, 1996; Barcala *et al.*, 2010). In this study, we provide strong evidence that the repression of a gene encoding an enzyme involved in lignin deposition/cross-linking is important for successful plant–nematode interaction, probably during GC establishment. This might also apply to other enzymes, as the process seems to be highly conserved between tomato and Arabidopsis. Given the striking amplitude and cross-species conservation of transcriptional down-regulation in incipient GCs, together with the increased expression of many genes involved in chromatin remodeling, it seems likely that cell fate manipulation through reprogramming of these genes is at the heart of the cell differentiation process triggered by nematodes. Their targeted over-expression or the identification of gain-of-function variants would provide additional tools for integrated nematode management in crops.

However, the transcriptional profiles of the genes putatively involved in the regulation of gene expression were not conserved between the two species (Figs 4, S4, Table S5), suggesting that gene networks or signaling cascades leading to downstream responses for GC differentiation and/or maintenance might diverge. This, together with the suggested high redundancy in plant targets for nematode effectors or in other plant proteins needed for feeding site development (Gheysen & Fenoll, 2011), could be part of the strategy of polyphagous nematodes able to infect most plant species.

Acknowledgements

References

Adie BA, Pérez-Pérez MM, Godoy MP, Sánchez-Serrano JJ, Schmelz EA, Solano R. 2007. ABA is an essential signal for plant resistance to pathogens affecting JA biosynthesis and the activation of defenses in Arabidopsis. *Plant Cell* 19: 1665–1681.

Almagro L, Gómez Ros LV, Belchi-Navarro S, Bru R, Ros Barceló A, Pedreño MA. 2009. Class III peroxidases in plant defence reactions. *Journal of Experimental Botany* 60: 377–390.

Aslam SN, Newman MA, Erbs G, Morrissey KL, Chinchilla D, Boller T, Jensen TT, De Castro C, Ierano T, Molinaro A et al. 2008. Bacterial polysaccharides suppress induced innate immunity by calcium chelation. *Current Biology* 18: 1078–1083.

Barcala M, Garcia A, Cabrera J, Casson S, Lindsey K, Favery B, Garcia-Casado G, Solano R, Fenoll C, Escobar C. 2010. Early transcriptomic events in microdissected Arabidopsis nematode-induced giant cells. *The Plant Journal* 61: 698–712.

Bar-Or C, Kapulnik Y, Koltai H. 2005. A broad characterization of the transcriptional profile of the compatible tomato response to the plant parasitic root knot nematode *Meloidogyne javanica*. *European Journal of Plant Pathology* 111: 181–192.

Bellafiore S, Shen Z, Rosso MN, Abad P, Shih P, Briggs SP. 2008. Direct identification of the *Meloidogyne incognita* secretome reveals proteins with host cell reprogramming potential. *PLoS Pathogens* 4: e1000192.

Benjamini Y, Hochberg Y. 1995. Controlling the False Discovery Rate: a practical and powerful approach to multiple testing. *Journal of the Royal Statistical Society* 57: 289–300.

Bhattarai KK, Xie QG, Mantelin S, Bishnoi U, Girke T, Navarre DA, Kaloshian I. 2008. Tomato susceptibility to root-knot nematodes requires an intact jasmonic acid signaling pathway. *Molecular Plant–Microbe Interactions* 21: 1205–1214.

Bhattarai KK, Atamian HS, Kaloshian I, Eulgem T. 2010. WRKY72-type transcription factors contribute to basal immunity in tomato and Arabidopsis as well as gene-for-gene resistance mediated by the tomato R gene *Mi-1*. *The Plant Journal* 63: 229–240.

Bird AF. 1961. The ultrastructure and histochemistry of a nematode-induced giant cell. *Journal of Biophysical and Biochemical Cytology* 11: 701–715.

Bird DM. 1996. Manipulation of host gene expression by root-knot nematodes. *Journal of Parasitology* 82: 881–888.

Bird DM, Wilson MA. 1994. DNA sequence and expression analysis of root-knot nematode-elicited giant cell transcripts. *Molecular Plant–Microbe Interactions* 7: 419–424.

Caillaud MC, Dubreuil G, Quentin M, Perfus-Barbeoch L, Lecomte P, de Almeida Engler J, Abad P, Rosso MN, Favery B. 2008b. Root-knot nematodes manipulate plant cell functions during a compatible interaction. *Journal of Physiology* 165: 104–113.

Caillaud MC, Lecomte P, Jammes F, Quentin M, Pagnotta S, Andrio E, de Almeida Engler J, Marfaing N, Gounon P, Abad P et al. 2008a. MAP65-3 microtubule-associated protein is essential for nematode-induced giant cell ontogenesis in Arabidopsis. *The Plant Cell* 20: 423–437.

Cardona A, Saalfeld S, Schindelin J, Arganda-Carreras I, Preibisch S, Longair M, Tomancak P, Hartenstein V, Douglas R. 2012. TrakEM2 software for neural circuit reconstruction. *PLoS ONE* 7: 1–8.

Casson S, Spencer M, Walker K, Lindsey K. 2005. Laser capture microdissection for the analysis of gene expression during embryogenesis of Arabidopsis. *The Plant Journal* 42: 111–123.

Chen Z, Zheng Z, Huang J, Lai Z, Fan B. 2009. Biosynthesis of salicylic acid in plants. *Plant Signaling & Behavior* 4: 493–496.

Cooper AJ, Latunde-Dada AO, Woods-Tor A, Lynn J, Lucas JA, Crute IR, Holub EB. 2008. Basic compatibility of *Albugo candida* in *Arabidopsis thaliana* and *Brassica juncea* causes broad-spectrum suppression of innate immunity. *Molecular Plant–Microbe Interactions* 21: 745–756.

Damiani I, Baldacci-Cresp F, Hopkins J, Andrio E, Balzergue S, Lecomte P, Puppo A, Abad P, Favery B, Hérouart D. 2012. Plant genes involved in harbouring symbiotic rhizobia or pathogenic nematodes. *New Phytologist* 194: 511–522.

De Almeida J, Favery B. 2011. Unravelling the plant cell cycle in nematode induced feeding sites. In: Jones J, Gheysen G, Fenoll C, eds. *Genomics and molecular genetics of plant–nematode interactions*. Dordrecht, the Netherlands: Springer, 349–368.

El Mansouri I, Mercado JA, Santiago-Domenech N, Pliego-Alfaro F, Valpuesta V, Quesada MA. 1999. Biochemical and phenotypical characterization of transgenic tomato plants over-expressing a basic peroxidase. *Physiologia Plantarum* 106: 355–362.

Escobar C, Sigal B, Mitchum M. 2011. Transcriptomic and proteomic analysis of the plant response to nematode infection. In: Jones J, Gheysen G, Fenoll C, eds. *Genomics and molecular genetics of plant–nematode interactions*. Dordrecht, the Netherlands: Springer, 157–176.

Eulgem T, Somssich IE. 2007. Networks of WRKY transcription factors in defense signaling. *Current Opinion in Plant Biology* 10: 366–371.

Fei Z, Joung JG, Tang X, Zheng Y, Huang M, Lee JM, McQuinn R, Tieman DM, Alba R, Klee HJ et al. 2011. Tomato functional genomics database: a comprehensive resource and analysis package for tomato functional genomics. *Nucleic Acids Research* 39: D1156–D1163.

Fosu-Nyarko J, Jones MG, Wang Z. 2009. Functional characterization of transcripts expressed in early-stage *Meloidogyne javanica*-induced giant cells isolated by laser microdissection. *Molecular Plant Pathology* 10: 237–248.

Fraser CM, Chapple C. 2011. The phenylpropanoid pathway in Arabidopsis. *The Arabidopsis Book* 9: e0152.

Gal TZ, Aussenberg ER, Burdman S, Kapulnik Y, Koltai H. 2006. Expression of a plant expansin is involved in the establishment of root knot nematode parasitism in tomato. *Planta* 224: 155–162.

Gamborg OL, Miller RA, Ojima K. 1968. Nutrient requirements of suspension cultures of soybean root cells. *Experimental Cell Research* 50: 151–158.

Gheysen G, Fenoll C. 2002. Gene expression in nematode feeding sites. *Annual Review of Phytopathology* 40: 191–219.

Gheysen G, Fenoll C. 2011. Arabidopsis as a tool for the study of plant–nematode interactions. In: Jones J, Gheysen G, Fenoll C, eds. *Genomics and molecular genetics of plant–nematode interactions*. Dordrecht, the Netherlands: Springer, 139–156.

Hammes UZ, Schachtman DP, Berg RH, Nielsen E, Koch W, McIntyre LM, Taylor CG. 2005. Nematode-induced changes of transporter gene expression in Arabidopsis roots. *Molecular Plant–Microbe Interactions* 18: 1247–1257.

Hewezi T, Howe PJ, Maier TR, Hussey RS, Mitchum MG, Davis EL, Baum TJ. 2010. Arabidopsis spermidine synthase is targeted by an effector protein of the cyst nematode *Heterodera schachtii*. *Plant Physiology* 152: 968–984.

Hewezi T, Maier T, Nettleton D, Baum T. 2012. The Arabidopsis MicroRNA396-GRF1/GRF3 regulatory module acts as a developmental regulator in the reprogramming of root cells during cyst nematode infection. *Plant Physiology* 159: 321–335.

Hollender C, Liu Z. 2008. Histone deacetylase genes in *Arabidopsis* development. *Journal of Integrative Plant Biology* 50: 875–885.

Huang GR, Dong AR, Davis EL, Baum TJ, Hussey RS. 2006. A root-knot nematode secretory peptide functions as a ligand for a plant transcription factor. *Molecular Plant–Microbe Interactions* 19: 463–470.

Huang X, Springer PS, Kaloshian I. 2003. Expression of the Arabidopsis *MCM* gene *PROLIFERA* during root-knot and cyst nematode infection. *Phytopathology* 93: 35–41.

Ithal N, Recknor J, Nettleton D, Maier T, Baum TJ, Mitchum MG. 2007. Developmental transcript profiling of cyst nematode feeding cells in soybean roots. *Molecular Plant–Microbe Interactions* 20: 510–525.

Ito T, Sun B. 2009. Epigenetic regulation of developmental timing in floral stem cells. *Epigenetics* 4: 564–567.

Jammes F, Lecomte P, de Almeida-Engler J, Bitton F, Martin-Magniette ML, Renou JP, Abad P, Favery B. 2005. Genome-wide expression profiling of the host response to root-knot nematode infection in *Arabidopsis*. *The Plant Journal* **44**: 447–458.

Jaouannet M, Perfus-Barbeoch L, Deleury E, Magliano M, Engler G, Vieira P, Danchin EGJ, Rocha MD, Coquillard P, Abad P *et al.* 2012. A root-knot nematode-secreted protein is injected into giant cells and targeted to the nuclei. *New Phytologist* **194**: 924–931.

Klink VP, Alkharouf N, MacDonald M, Matthews B. 2005. Laser capture microdissection (LCM) and expression analyses of *Glycine max* (soybean) syncytium containing root regions formed by the plant pathogen *Heterodera glycines* (soybean cyst nematode). *Plant Molecular Biology* **59**: 965–979.

Klink VP, Hosseini P, Alkharouf N, Matthews B. 2009. A gene expression analysis of syncytia laser microdissected from the roots of the *Glycine max* (soybean) genotype PI 548402 (Peking) undergoing a resistant reaction after infection by *Heterodera glycines* (soybean cyst nematode). *Plant Molecular Biology* **71**: 525–567.

Klink VP, Overall C, Alkharouf N, MacDonald M, Matthews B. 2007. Laser capture microdissection (LCM) and comparative microarray expression analysis of syncytial cells isolated from incompatible and compatible soybean (*Glycine max*) roots infected by the soybean cyst nematode (*Heterodera glycines*). *Planta* **226**: 1389–1409.

Klink VP, Overall C, Alkharouf N, MacDonald M, Matthews B. 2010. Microarray detection call methodology as a means to identify and compare transcripts expressed within syncytial cells from soybean (*Glycine max*) roots undergoing resistant and susceptible reactions to the soybean cyst nematode (*Heterodera glycines*). *Journal of Biomedicine and Biotechnology* **2010**: 1–30.

Knizewski L, Ginalski K, Jerzmanowski A. 2008. Snf2 proteins in plants: gene silencing and beyond. *Trends in Plant Science* **13**: 557–565.

Kohler C, Hennig L, Bouveret R, Gheyselinck J, Grossniklaus U, Gruissem W. 2003. *Arabidopsis* MSI1 is a component of the MEA/FIE *Polycomb* group complex and required for seed development. *The Embo Journal* **22**: 4804–4814.

Koltai H, Bird DM. 2000. Epistatic repression of *PHANTASTICA* and class 1 *KNOTTED* genes is uncoupled in tomato. *The Plant Journal* **22**: 455–459.

Koltai H, Dhandaydham M, Opperman C, Thomas J, Bird D. 2001. Overlapping plant signal transduction pathways induced by a parasitic nematode and a rhizobial endosymbiont. *Molecular Plant–Microbe Interactions* **14**: 1168–1177.

Lindroth AM, Cao X, Jackson JP, Zilberman D, McCallum CM, Henikoff S, Jacobsen SE. 2001. Requirement of *CHROMOMETHYLASE3* for maintenance of CpXpG methylation. *Science* **292**: 2077–2080.

Lucena MA, Romero-Aranda R, Mercado JA, Cuarteros J, Valpuesta V, Quesada MA. 2003. Structural and physiological changes in the roots of tomato plants over-expressing a basic peroxidase. *Physiologia Plantarum* **118**: 422–429.

Maunoury N, Redondo-Nieto M, Bourcy M, Van de Velde W, Alunni B, Laporte P, Durand P, Agier N, Marisa L, Vaubert D *et al.* 2010. Differentiation of symbiotic cells and endosymbionts in *Medicago truncatula* nodulation are coupled to two transcriptome-switches. *PLoS ONE* **5**: e9519.

Moreau S, Verdenaud M, Ott T, Letort SB, de Billy FO, Niebel A, Gouzy JM, Carvalho-Niebel F, Gamas P. 2011. Transcription reprogramming during root 712 nodule development in *Medicago truncatula*. *PLoS ONE* **6**: e16463.

Olsen AN, Ernst HA, Leggio LL, Skriver K. 2005. NAC transcription factors: structurally distinct, functionally diverse. *Trends in Plant Science* **10**: 79–87.

Passardi F, Theiler G, Zamocky M, Cosio C, Rouhier N, Teixera F, Margis-Pinheiro M, Ioannidis V, Penel C, Falquet L *et al.* 2007. PeroxiBase: the peroxidase database. *Phytochemistry* **68**: 1605–1611.

Portillo M, Fenoll C, Escobar C. 2006. Evaluation of different RNA extraction methods for small quantities of plant tissue: combined effects of reagent type and homogenization procedure on RNA quality-integrity and yield. *Physiologia Plantarum* **128**: 1–7.

Portillo M, Lindsey K, Casson S, Garcia-Casado G, Solano R, Fenoll C, Escobar C. 2009. Isolation of RNA from laser-capture-microdissected giant cells at early differentiation stages suitable for differential transcriptome analysis. *Molecular Plant Pathology* **10**: 523–535.

Rosso M-N, Grenier E. 2011. Other nematode effectors and evolutionary constraints. In: Jones J, Gheysen G, Fenoll C, eds. *Genomics and molecular genetics of plant–nematode interactions*. Dordrecht, the Netherlands: Springer, 287–307.

Saeed AI, Bhagabati NK, Braisted JC, Liang W, Sharov V, Howe EA, Li J, Thiagarajan M, White JA, Quackenbush J. 2006. TM4 microarray software suite. *Methods in Enzymology* **411**: 134–193.

Sanchez MdeL, Caro E, Desvoyes B, Ramirez-Parra E, Gutierrez C. 2008. Chromatin dynamics during the plant cell cycle. *Seminars in Cell and Developmental Biology* **19**: 537–546.

Sawa S, Demura T, Horiguchi G, Kubo M, Fukuda H. 2005. The *ATE* genes are responsible for repression of transdifferentiation into xylem cells in Arabidopsis. *Plant Physiology* **137**: 141–148.

Schaff JE, Nielsen DM, Smith CP, Scholl EH, Bird DM. 2007. Comprehensive transcriptome profiling in tomato reveals a role for glycosyltransferase in *Mi*-mediated nematode resistance. *Plant Physiology* **144**: 1079–1092.

Schlink K. 2010. Down-regulation of defense genes and resource allocation into infected roots as factors for compatibility between *Fagus sylvatica* and *Phytophthora citricola*. *Functional & Integrative Genomics* **10**: 253–264.

Shultz RW, Tatineni VM, Hanley-Bowdoin L, Thompson WF. 2007. Genome-wide analysis of the core DNA replication machinery in the higher plants Arabidopsis and rice. *Plant Physiology* **144**: 1697–1714.

Siefers N, Dang KK, Kumimoto RW, Bynum WE, Tayrose G, Holt BF. 2009. Tissue-specific expression patterns of Arabidopsis NF-Y transcription factors suggest potential for extensive combinatorial complexity. *Plant Physiology* **149**: 625–641.

Smant G, Jones J. 2011. Suppression of plant defences by nematodes. In: Jones J, Gheysen G, Fenoll C, eds. *Genomics and molecular genetics of plant–nematode interactions*. Dordrecht, the Netherlands: Springer, 273–286.

Smith LM, Pontes O, Searle I, Yelina N, Yousafzai FK, Herr AJ, Pikaard CS, Baulcombe DC. 2007. An SNF2 protein associated with nuclear RNA silencing and the spread of a silencing signal between cells in *Arabidopsis*. *The Plant Cell* **19**: 1507–1521.

Smyth GK. 2004. Linear models and empirical Bayes methods for assessing differential expression in microarray experiments. *Statistical Applications in Genetics and Molecular Biology* **3**: 1–26.

Smyth GK, Speed T. 2003. Normalization of cDNA microarray data. *Methods* **31**: 265–273.

Starr JL. 1993. Dynamics of the nuclear complement of giant cells induced by *Meloidogyne incognita*. *Journal of Nematology* **25**: 416–421.

Szakasits D, Heinen P, Wieczorek K, Hofmann J, Wagner F, Kreil DP, Sykacek P, Grundler FM, Bohlmann H. 2009. The transcriptome of syncytia induced by the cyst nematode *Heterodera schachtii* in Arabidopsis roots. *The Plant Journal* **57**: 771–784.

Toledo-Ortiz G, Huq E, Quail PH. 2003. The Arabidopsis basic/helix-loop-helix transcription factor family. *The Plant Cell* **15**: 1749–1770.

Truman W, de Zabala MT, Grant M. 2006. Type III effectors orchestrate a complex interplay between transcriptional networks to modify basal defence responses during pathogenesis and resistance. *The Plant Journal* **46**: 14–33.

Urbanczyk-Wochniak E, Usadel B, Thimm O, Nunes-Nesi A, Carrari F, Davy M, Blasing O, Kowalczyk M, Weicht D, Polinceusz A *et al.* 2006. Conversion of MapMan to allow the analysis of transcript data from Solanaceous species: effects of genetic and environmental alterations in energy metabolism in the leaf. *Plant Molecular Biology* **60**: 773–792.

Wang Z, Potter RH, Jones MGK. 2001. A novel approach to extract and analyse cytoplasmic contents from individual giant cells in tomato roots induced by *Meloidogyne javanica*. *International Journal of Nematology* **11**: 219–225.

Wang Z, Potter RH, Jones MGK. 2003. Differential display analysis of gene expression in the cytoplasm of giant cells induced in tomato roots by *Meloidogyne javanica*. *Molecular Plant Pathology* **4**: 361–371.

Williamson VM, Hussey RS. 1996. Nematode pathogenesis and resistance in plants. *The Plant Cell* **8**: 1735–1745.

Zhong R, Lee C, Zhou J, McCarthy RL, Ye ZH. 2008. A battery of transcription factors involved in the regulation of secondary cell wall biosynthesis in Arabidopsis. *The Plant Cell* **20**: 2763–2782.

Supporting Information

Additional supporting information may be found in the online version of this article.

Fig. S1 Microarray-based temporal changes of gall differentially expressed genes (DEGs).

Fig. S2 Overview of gall differentially expressed genes (DEGs) classified in functional categories by Mapman.

Fig. S3 Summary of exclusive and co-expressed differentially expressed genes (DEGs) between giant cells (GCs) and galls classified by Mapman.

Fig. S4 Mapman map fitting of differentially expressed genes (DEGs) related to 'RNA-regulation of transcription' in galls and giant cells (GCs).

Fig. S5 *In situ* reverse transcription-polymerase chain reaction (RT-PCR) hybridization of uninfected root longitudinal sections as controls.

Table S1 List of giant cell (GC)-distinctive differentially expressed genes (DEGs) with a fold change (FC) > 1.9 and < -1.9

Table S2. Examples of giant cell (GC) differentially expressed genes (DEGs) from different categories (Mapman)

Table S3 Detailed information of TBLASTN and TBLASTX reciprocal analysis

Table S4 Interactive search of tomato–Arabidopsis homologous differentially expressed genes (DEGs) in giant cells (GCs)

Table S5 List of Arabidopsis–tomato transcription factors homologs

Table S6 ID Interactive tomato gene finder of giant cell (GC) and gall differentially expressed genes (DEGs) as a function of the infection stage

Table S7 List of gall-exclusive differentially expressed genes (DEGs) at 1 d post-infection (dpi)

Table S8 Examples of gall differentially expressed genes (DEGs) from different categories (Mapman)

Table S9 Examples of exclusive and co-regulated genes in galls and giant cells (GCs) by Mapman

Table S10 List of distinctive giant cell (GC) genes

Table S11 List of genes with opposite expression patterns in giant cells (GCs) and galls

Table S12 Primers used for quantitative reverse transcription-polymerase chain reaction (qRT-PCR), *in situ* PCR analysis and microarray sample labeling

Table S13 List of differentially expressed genes (DEGs) with no uniform pattern during infection in galls and giant cells (GCs)

Please note: Wiley-Blackwell are not responsible for the content or functionality of any supporting materials supplied by the authors. Any queries (other than missing material) should be directed to the corresponding author for the article.

About *New Phytologist*

- *New Phytologist* is an electronic (online-only) journal owned by the New Phytologist Trust, a **not-for-profit organization** dedicated to the promotion of plant science, facilitating projects from symposia to free access for our Tansley reviews.

- Regular papers, Letters, Research reviews, Rapid reports and both Modelling/Theory and Methods papers are encouraged.
  We are committed to rapid processing, from online submission through to publication 'as ready' via *Early View* – our average time to decision is <25 days. There are **no page or colour charges** and a PDF version will be provided for each article.

- The journal is available online at Wiley Online Library. Visit **www.newphytologist.com** to search the articles and register for table of contents email alerts.

- If you have any questions, do get in touch with Central Office (np-centraloffice@lancaster.ac.uk) or, if it is more convenient, our USA Office (np-usaoffice@ornl.gov)

- For submission instructions, subscription and all the latest information visit **www.newphytologist.com**